Available online at www.sciencedirect.com
ScienceDirect
Trans. Nonferrous Met. Soc. China 25(2015) 981−990
Transactions of Nonferrous Metals Society of China
www.tnmsc.cn

Synthesis of platy potassium magnesium titanate and its application in removal of copper ions from aqueous solution

Yan-ni TAN, Ni SONG, Yong LIU, Tao LUO, Yu-hai DOU, Qing ZHANG, Qian-nan LIU, Lan-lan LUO

State Key Laboratory of Powder Metallurgy, Central South University, Changsha 410083, China

Received 5 December 2013; accepted 21 November 2014

Abstract: Platy potassium magnesium titanate ($K_{0.8}Mg_{0.4}Ti_{1.6}O_4$, KMTO) was synthesized by a flux method. The potential application of KMTO in removing copper ions from water pollutants was investigated. The crystal phases of specimens were identified by XRD. The morphology and structural information were characterized by SEM and TEM. The adsorption behavior under different conditions was investigated, including different pH values and different initial copper ion concentrations. The results show that the maximum adsorption capacity of Cu(II) ions is 290.697 mg/g, and almost 99.9% of Cu(II) ions can be removed, which is much higher than that of other sorbents reported. The kinetics of KMTO for the adsorption of Cu(II) ions was studied and the best fit can be obtained by the pseudo-second-order model. Adsorption isothermal data can be well interpreted by the Freundlich equation (R^2=0.991). In conclusion, this study highlights that KMTO is a potential material for the efficient removal of heavy metal ions in polluted water. It also opens up a new opportunity for the applications of platy KMTO.

Key words: potassium magnesium titanate; waste water; copper ion; removal; adsorption kinetics; flux method

1 Introduction

Increased industrialization and urbanization in modern society may bring about serious water contamination of heavy metals. Copper is one of the widely used heavy metals in modern industries, such as metal plating, mining, battery manufacturing, paints and pigment production, and glass production [1]. Its applications often result in harmful effects on aquatic ecosystems due to its non-biodegradable and persistent nature [2,3]. Intake of excessively large doses of copper can cause severe mucosal irritation and corrosion, widespread capillary damage, hepatic and renal damage, central nervous system irritation followed by depression, kidney damage, anemia and even coma, and eventual death [1,4]. According to the US Environmental Protection Agency (EPA) and the World Health Organization (WHO), the permissible levels for copper in drinking water are 1.3 and 2 mg/L, respectively [5]. Therefore, the removal of copper from wastewater has become a very important environmental issue.

Many methods have been proposed for the removal of heavy metals including copper ions, such as chemical precipitation, adsorption, solvent extraction, evaporation and electrodialysis [1]. Among these methods, the ion-exchange adsorption is the most commonly used process, because it is a relatively clean (without need for extra disposal) and energy efficient method, and has a high selectivity for certain ions even in solutions of low concentration of the target ion [6−9]. Furthermore, it can be utilized in metal recovery and water reuse, which are of economical importance. Though various substances, such as clay minerals, phosphate, hydrous metal oxides, silicate and zeolite have been widely used as ion exchangers, there are still some problems limiting their applications, such as the impurities in the adsorbents, slow adsorption kinetics, low adsorption capacities, or high cost [10−14]. Consequently, it is important to explore low cost and abundant materials that have high efficiency in removing heavy ions from industrial wastewater.

Lepidocrocite type titanates ($A_xTi_{2-y}M_yO_4$, where A is an interlayer alkali metal ion, and M is metal ion or vacancy) have a wide range in chemical composition. The metal ions or vacancies occupy the octahedral sites

Foundation item: Project (51272289) supported by the National Natural Science Foundation of China; Project (51021063) supported by the Creative Research Group of National Science Foundation of China
Corresponding author: Yong LIU; Tel: +86-731-88836939; Fax: +86-731-88710855; E-mail: yonliu@csu.edu.cn
DOI: 10.1016/S1003-6326(15)63688-3

in the base layers, and substitute the Ti^{4+} ions in the nominal [MO_2] framework. The substitution gives a negative charge balanced by interlayer alkali ion [15]. The relatively wide inter-layer space and low negative charge density of the host layer compared with other titanates are responsible for many excellent properties, such as good swelling properties, catalytic properties and intercalation reactivity [16−19]. In addition, the interlayer ions and metal ions of lepidocrocite type titanates are exchangeable with a variety of inorganic and organic cations, resulting in an excellent ion-exchange property. Lepidocrocite-related titanates have been successfully used in many applications, such as photocatalysts, semiconductor materials, adiabatic materials, UV-shielding materials, cation-exchangers and functional filling materials. They also have the potential to be used as effective adsorbents for removing heavy metals from waste water [20,21]. Furthermore, good mechanical property of ceramic materials also facilitates them to be used in bulk adsorption systems.

Potassium magnesium titanate ($K_{0.8}Mg_{0.4}Ti_{1.6}O_4$, KMTO) is well-known for its ion-exchange property due to its unique atomic structure. However, platy KMTO was widely used as reinforcement in friction materials [22], and it has not been used in ion-exchange in solutions. However, so far few studies have been reported about the synthesis and characterization of platy KMTO. Also, as we know, no paper has reported about the application of platy KMTO in removing copper ions from waste water. In this work, platy lepidocrocite type KMTO was prepared and characterized. And its application in removing copper ions from aqueous solution was investigated.

2 Experimental

2.1 Preparation of KMTO

The platy KMTO was prepared by a flux (molten salt) method. The method consists of adding precursors at the required ratio to a molten salt mixture often close to a eutectic stoichiometry, which accelerates the kinetics of formation of the desired compounds [23]. All the chemicals used in this work were of analytical grade and purchased from Xilong Chemical Co., Ltd., China. The starting materials were K_2CO_3, $Mg(OH)_2$ and TiO_2 (n(Ti):n(K):n(Mg)=4.1:2:1) mixed with an appropriate amount of KCl flux. The mixture was ground and calcined at 1050 °C for 3 h. After furnace cooling, the obtained powder was washed with boiling pure water to remove the KCl flux and then dried at 80 °C for 12 h in the drying oven.

2.2 Characterization of KMTO

Crystal phases of specimens were identified using a powder X-ray diffractometer (XRD, D/ruax 2550PC, Japan). Morphology and structural information were obtained using a field emission scanning electron microscope (FESEM, NOVA NANOSEM 230, USA) and a field emission transmission electron microscope (FETEM, JEOL JEM−2100F, Japan).

2.3 Adsorption experiments

In order to determine the influence of time, pH and initial concentration of Cu(II) ions on the sorption capacity of KMTO for Cu(II) ions, batches of experiments were carried out. 0.3 g KMTO was added to 100 mL of $Cu(OH)_2$ solution, with preselected concentrations and pH values. The solutions were stirred at 150 r/min and (293±2) K for a predetermined period in a shaking incubator. After stirring for different time, the suspensions were filtered using filter flask and filter paper (Whatman, grade 1). The final Cu(II) ion concentrations in the filtrates as well as in the initial solution were determined by an inductively coupled plasma (ICP, IRIS Advantage 1000, USA). The amount of Cu(II) ions adsorbed at equilibrium q_e (mg/g), and the metal ion removal rate R (%), were calculated by Eqs. (1) and (2), respectively:

$$q_e = \frac{(C_i - C_e)V}{m} \tag{1}$$

$$R = \frac{C_i - C_e}{C_i} \times 100\% \tag{2}$$

where C_i is the initial concentration of metal ions in the aqueous solution (mg/L); C_e is the equilibrium concentration of metal ions in the aqueous solution (mg/L); m is the mass of KMTO (g); V is the the volume of sample (L).

2.3.1 Adsorption kinetics

For kinetics measurements, 0.3 g KMTO was added into 100 mL of $Cu(OH)_2$ solution with initial concentration of 100 mg/L (determined by ICP). Then, the suspensions were shaken in different time intervals ranging from 5 to 400 min, filtrated and analyzed to determine the concentration of Cu(II) ions.

2.3.2 Effect of pH

The effect of pH was studied in the range of 1.0−9.0. The initial Cu(II) ion concentration was 100 mg/L (determined by ICP), and the initial pH values were adjusted by adding aqueous ammonia and HNO_3 solution. After 6 h of adsorption, the suspensions were filtrated, and analyzed for the final Cu(II) ion concentrations.

2.3.3 Effect of initial Cu(II) ion concentration

For determining the isotherms of adsorption metal ions, 0.3 g KMTO was added into 100 mL of $Cu(OH)_2$ solution with different concentrations (from 100 to 550 mg/L). The suspensions were then filtrated after 6 h of

adsorption, and the concentration of Cu(II) ions was detected by ICP.

3 Results and discussion

3.1 Preparation of platy KMTO

Figure 1 shows the XRD pattern of sample prepared by the flux method. It can be observed that the main phase is $K_{0.8}Mg_{0.4}Ti_{1.6}O_4$ (PDF No. 73−0671). And its peak intensity is strong, indicating a good crystallinity. The low intensity diffraction peaks are assigned to $K_2Ti_4O_9$ (PDF No. 32−0861), and the formation of which may have been caused by a small deficiency of magnesium due to the evaporation of magnesium oxide.

Typical SEM and TEM images of the products are shown in Fig. 2. It is clear that the powders are regular plates of different sizes, with diameter of 0.3−5 μm, thickness of 15 nm (Figs. 2(a) and (b)). From the TEM image (Fig. 2(c)), it can be also observed that the powders are plate-like, and the surface of powder is smooth. An individual plate was selected and tilted to obtain corresponding selected-area electron diffraction patterns (SAED). The crystal is found to have a relatively high crystallinity as the highly ordered SAED spots can clearly be observed (Fig. 2(d)). The SAED pattern shows obvious lepidocrocite-related electron diffraction, and lattice spacings are 3.63 and 3.61 Å,

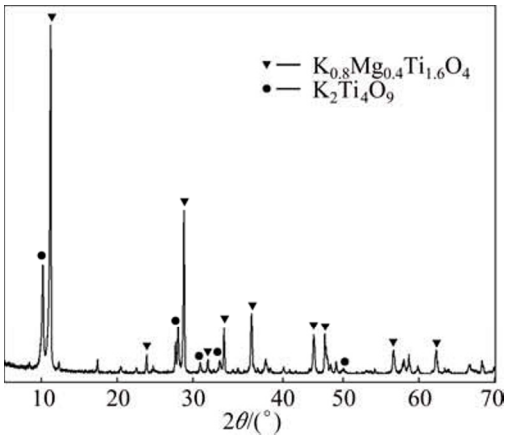

Fig. 1 XRD pattern of sintering KMTO powder at molar ratio of Ti to K being 2.05:1 and calcined at 1050 °C for 3 h

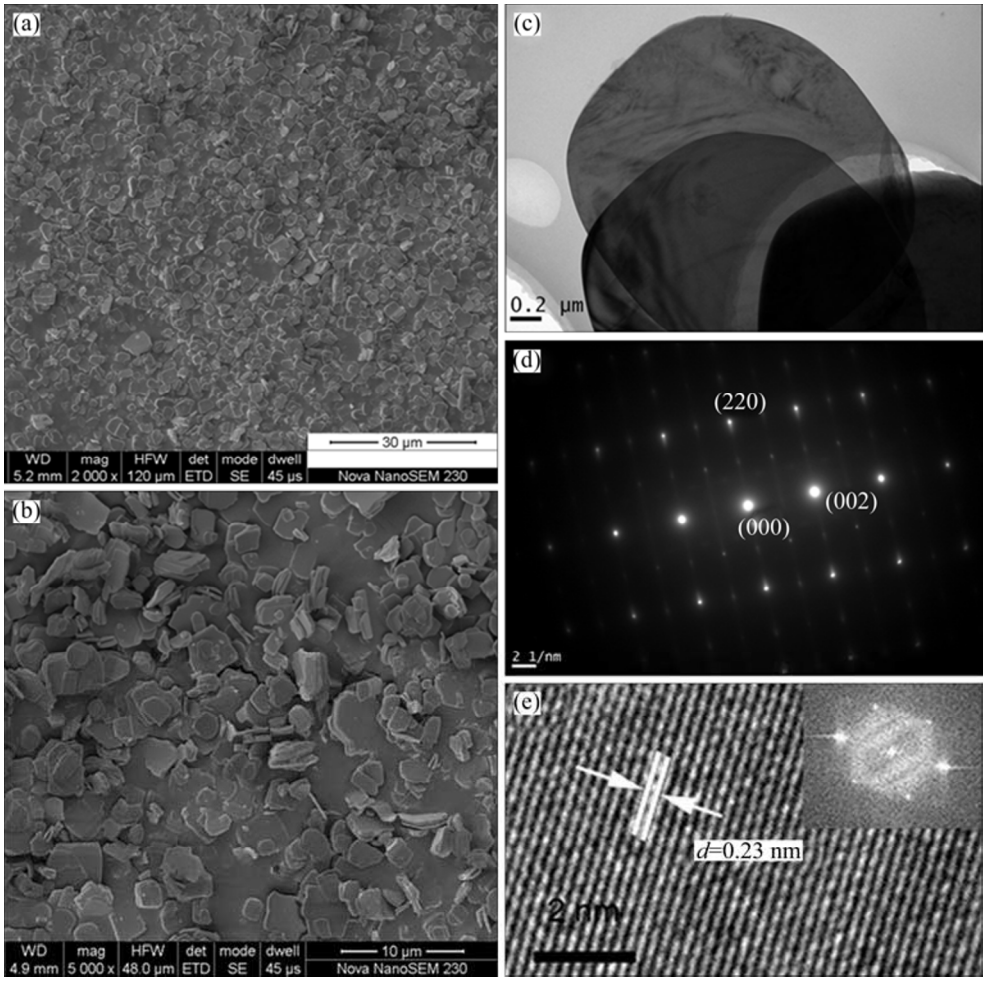

Fig. 2 SEM and TEM images of sintering KMTO powders at molar ratio of Ti to K being 2.05:1 and calcined at 1050 °C for 3 h: (a, b) SEM image; (c) TEM image; (d) Selected area electron diffraction (SAED); (e) HRTEM image and its Fourier transform

respectively, which correspond to the (110) and (202) interplanar spacing of the orthorhombic $K_{0.8}Mg_{0.4}Ti_{1.6}O_4$. Figure 2(e) shows the corresponding HRTEM image. It shows that the fringe spacing is 0.23 nm, corresponding to the (111) interplanar distance of the orthorhombic $K_{0.8}Mg_{0.4}Ti_{1.6}O_4$. It also reveals that the growth plane of the nanoribbons is (111). Furthermore, the HRTEM image further demonstrates that the $K_{0.8}Mg_{0.4}Ti_{1.6}O_4$ is single crystal with very good crystallinity. From the Fourier transform of the image, the growth orientation of the nanoribbon is determined to be [010] crystallographic direction.

3.2 Formation mechanism of KMTO

In this work, well-developed $K_{0.8}Mg_{0.4}Ti_{1.6}O_4$ crystals for use as heavy-ion sorbent were successfully synthesized by a flux method, which is similar to but not the same as that in our previous work [24]. The specific conditions are different. The method is environmentally friend, simple, and low-cost, and can produce binary or multicomponent crystals at temperatures below the melting points of the solutes. Potassium chloride (KCl) was chosen as the molten salt because it is low-cost and harmless to human beings and the environment. In addition, it can provide K^+ ions to compensate the evaporation loss of potassium oxide in course of heat treatment [25].

$K_{0.8}Mg_{0.4}Ti_{1.6}O_4$ plates were synthesized in KCl molten salt at 1050 °C, which is much lower than the melting point of the raw material TiO_2. Thus, conventional vapor–liquid–solid (VLS) or vapor–solid (VS) mechanism cannot be used to interpret the growth of $K_{0.8}Mg_{0.4}Ti_{1.6}O_4$ plates. The formation of $K_{0.8}Mg_{0.4}Ti_{1.6}O_4$ is probably based on the oriented attachment mechanism [26,27]. It involves spontaneous self-organization of adjacent particles so that they share a common crystallographic orientation, followed by the connection of these particles at a planar interface. This mechanism is relevant in cases where particles are free to move (such as in solution or where particles have abundant surface-bound water). In the growth process of $K_{0.8}Mg_{0.4}Ti_{1.6}O_4$ nuclei, molten KCl can provide a flexible liquid environment for $K_{0.8}Mg_{0.4}Ti_{1.6}O_4$ crystals to grow in an unconstrained manner. That is, they can grow freely from mechanical or thermal constraints into solution, and therefore develop into plates. It can be assumed that K^+ and Mg^{2+}, which are from the molten salt, come into the TiO_2 matrix along (111) crystallographic plane and form the layered structure $K_{0.8}Mg_{0.4}Ti_{1.6}O_4$. Then, the thin layers align in almost the same direction and fuse together, leading to the formation of thick plates.

3.3 Adsorption behaviors

3.3.1 Adsorption kinetics

The adsorption rate was studied using $Cu(OH)_2$ solution with an initial Cu(II) ion concentration of 100 mg/L and pH of 3.0, as shown in Fig. 3(a). The adsorption maintained at a very high efficiency during the initial 5 min, and 81.3% of Cu(II) ion was removed from the solution. Thereafter, the reaction rate decreased gradually, and the adsorption reached equilibrium at approximately 350 min, when about 99.9% of Cu(II) ion was removed. These results suggest that the adsorption of metal cations takes place as a gradual process. It is

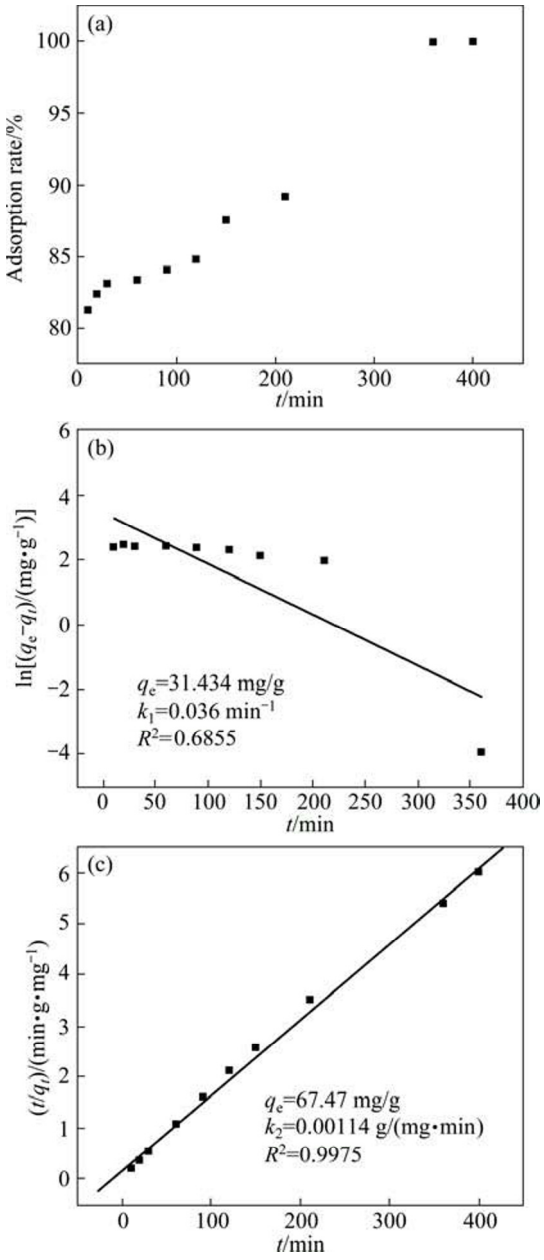

Fig. 3 Effect of contact time on adsorption rate of KMTO (a), kinetic parameters and pseudo-first-order kinetic isotherm (b) and pseudo-second-order kinetic isotherm (c) for adsorption of Cu(II) ions by KMTO at pH 3.0, 30 °C and initial Cu(II) ion concentration of 100 mg/L

possible that during the initial stage, the coverage of active adsorption sites was low and the adsorbed ions rapidly occupied the sites in a random manner, resulting in a higher rate of uptake.

Lagergren's pseudo-first-order and pseudo-second-order kinetic models were used to predict the adsorption behavior of Cu(II) ions as function of time using the adsorption data. The pseudo-first-order kinetic model is expressed in the following linear form [28]:

$$\ln(q_e-q_t)=\ln q_e-k_1t \quad (3)$$

where q_e and q_t (mg/g) are the amounts of metal ion adsorbed at equilibrium and contact time t (min), respectively; k_1 (min^{-1}) is the pseudo-first-order rate constant. k_1 and q_e can be respectively computed from the slope and intercept of the plot of $\ln(q_e-q_t)-t$.

The pseudo-second-order kinetic model is described by [28]

$$\frac{t}{q_t}=\frac{1}{k_2q_e^2}+\frac{1}{q_e}t \quad (4)$$

where k_2 (g/(mg·min)) is the pseudo-second-order rate constant. The values of k_2 and q_e can be respectively calculated from the slope and intercept of the plot of t/q_t-t. The pseudo-first-order model is the first equation for the adsorption of liquid/solid system based on solid capacity and is generally applicable over the initial stage of the adsorption process. The pseudo-second-order model is more suitable for the prediction of the behavior over the whole range of adsorption when the chemisorption mechanism is the rate-limiting step [29]. The linear fit and the kinetic parameters of pseudo-first-order model and pseudo-second-order model are shown in Figs. 3(b) and (c). It is evident that the uptake of Cu(II) ions for KMTO can be explained using the pseudo-second-order model with the higher value of correlation coefficient (typically, R^2>0.99) but not the pseudo-first-order model (R^2=0.6855). The result suggests that the overall rate of the adsorption process was controlled by chemical adsorption in the case of Cu(II) ions [29−31].

3.3.2 Effects of pH on removal of Cu(II) ions with KMTO

The pH value of the aqueous solution has been identified as the most important parameter during adsorption process. It can significantly affect the surface charge of absorbents, the metal ionization degree and the metal speciation, and thus, the adsorption mechanism and the uptake capacity. This is partly because hydrogen ions themselves strongly compete with heavy metal ions for the adsorption sites. So, the effect of initial pH (1.0−9.0) on adsorption of Cu(II) ions was studied, as shown in Fig. 4(a). It can be seen that the adsorption rate of Cu(II) ions is relatively low under strong acidic condition (pH=1) accounting for 49.2%, followed by a marked rise to 99% at pH of 3.0. Thereafter, the adsorption rate slightly deceases at pH between 4.0 and 7.0, and then increases again at pH of 9.0. A better performance of adsorbent is obtained when the pH value of acid solution is 3.0.

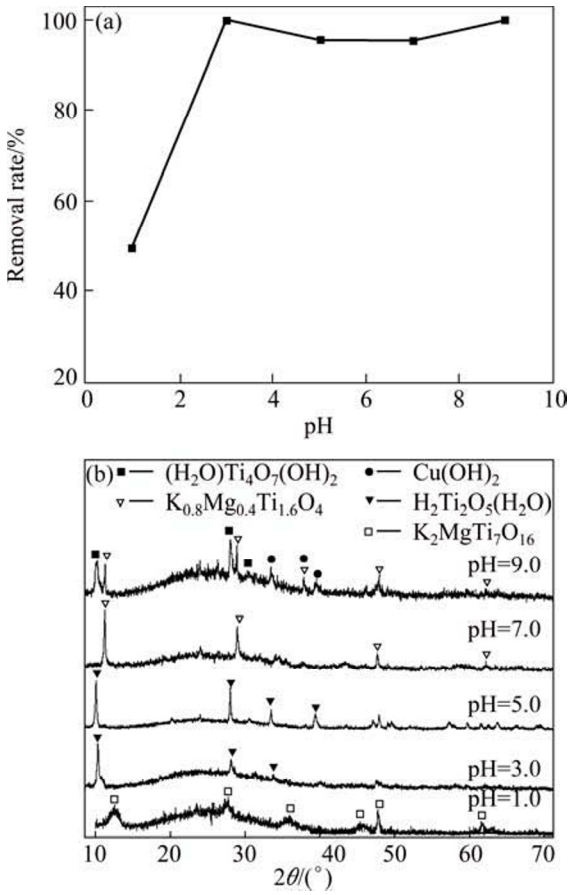

Fig. 4 Effect of pH on Cu(II) ion removal rate of KMTO at 30 °C and initial Cu(II) ion concentration of 200 mg/L (a) and XRD patterns of KMTO powders after adsorption of Cu(II) ions at different pH values (b)

The effect of pH on adsorption of Cu(II) ions can be reasonably explained by the electrostatic potential on the surface of KMTO. The zero potential for KMTO is found to be at pH=2.14, thus, electrostatic repulsion occurs between Cu(II) ions and the adsorbent surface at pH<3.0, resulting in a low uptake of Cu(II) ions. When the pH value is between 3.0 and 7.0, the surfaces of KMTO become negatively charged. Therefore, the adsorption rate of Cu(II) ions is enhanced due to the electrostatic attraction.

At pH=3.0−7.0, the adsorption rate decreases gradually with increasing pH value, which may be caused by the change of copper speciation. According to previous studies [32,33], Cu^{2+} ions are predominant at pH values below 5.0. However, besides Cu^{2+}, a high content of $[CuOH]^+$ and $[Cu_2(OH)_2]^{2+}$, formed by the reaction between Cu^{2+} and H_2O, can also be found at pH

between 5.0 and 7.0. As pH increases, more $[CuOH]^+$ and $[Cu_2(OH)_2]^{2+}$ are generated. This may not be a favorable change for the adsorption. And the adsorbents are deteriorated with copper precipitation, thus the adsorption rate decreases. At pH=9.0, the adsorption rate experiences an increase which may be caused by the precipitation reaction between Cu^{2+} and OH^-.

Figure 4(b) illustrates the XRD patterns of KMTO after adsorbing Cu(II) ions, which can also help to understand the adsorption process. At pH=1.0, the crystal phase of obtained sample is indexed as $K_2MgTi_7O_{16}$ (PDF No. 18−1032), which is another type of potassium magnesium titanate with a tunnel structure. Therefore, it is deduced that the incorporation of strong acid may destroy the symmetry of $K_{0.8}Mg_{0.4}Ti_{1.6}O_4$, resulting in the change of structure from layered to tunnel structure. Because exchangeable K^+ ions are enclosed within the tunnels and not easily accessible for exchange, $K_2MgTi_7O_{16}$ shows poor ion exchange properties [34]. Generally, it is the combination of the surface charge and the tunnel structure that result in the lowest removal rate at pH=1.0. When pH values increase to 3.0 and 5.0 respectively, the main phases are identified as $H_2Ti_2O_5(H_2O)$ (PDF No. 47−0124), which belongs to the same crystal system (orthorhombic) as $K_{0.8}Mg_{0.4}Ti_{1.6}O_4$, indicating that ion exchange is an in-situ reaction. In acid solution, there is a competition between H^+ and Cu^{2+} for the sorption sites. As the initial concentration of Cu^{2+} is far lower than that of H^+, most adsorption sites of KMTO are occupied by H^+. Therefore, the main phases of most final ion-change products are not copper-related compounds. As pH increases to 7.0, the final phase is not changed and indexed as $K_{0.8}Mg_{0.4}Ti_{1.6}O_4$. The ion-exchange reaction mainly occurs between Cu^{2+} and K^+ ions because fewer H^+ ions are available to compete with Cu^{2+} ions for adsorption sites. The mixture of titanium aqua oxide hydroxide ($(H_2O)Ti_4O_7(OH)_2$, PDF No. 38−0699) and $Cu(OH)_2$ (PDF No. 03−0310) are found at pH=9.0. The metal ions would be associated with ammonium ions to form precipitate on the surface of KMTO or transport in the space between sorbent particles, resulting in an enhancement of removal rate.

3.3.3 Effect of initial ion concentration

The metal adsorption is particularly dependent on the initial ion concentration. At low concentration, metals are absorbed to specific sites which will be saturated and occupied with increasing metal concentration [4]. To study the effect of the initial Cu(II) ion concentrations on removal rate by KMTO, different Cu(II) ion concentrations from 100 to 550 mg/L were used at adsorption time of 6 h. The results are presented in Fig. 5. It is shown that the adsorption capacity of KMTO increases and the removal rate of Cu(II) ions decreases with increasing initial concentration of Cu(II) ions. At the lower concentrations (100, 200 and 300 mg/L, respectively), the removal rates are very high (99.9%, 99.2% and 94.9%, respectively) and the adsorption capacities of KMTO increase linearly (66.62, 132.27 and 189.87 mg/L). This is because the adsorption is not saturated at low initial concentrations of Cu(II) ions. When the initial concentration increases continuously, the removal rates are only 84.9% and 82.1% at the concentrations of 400 and 500 mg/L, respectively. The adsorption capacity increases with increasing initial concentration, because the ratio of the initial number of copper ions to the exchangeable potassium ions and the available adsorption surface area are high.

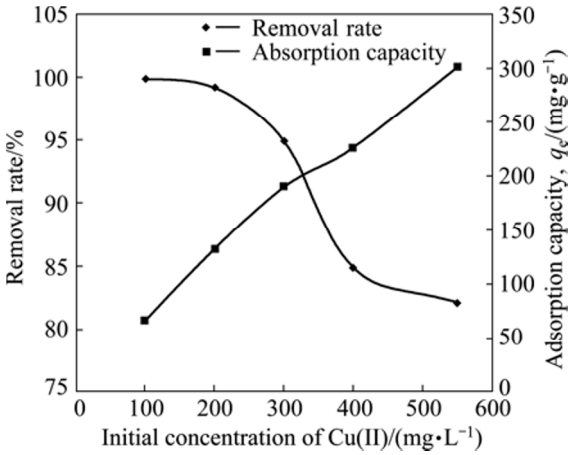

Fig. 5 Effect of initial concentration of Cu(II) ions on removal rate and adsorption capacity of KMTO at 30 °C, pH=3.0 and adsorption time of 6 h

3.3.4 Adsorption isotherms of Cu(II) ions

Adsorption isotherms show the relationship between the metal concentration in solution and the amount of metal adsorbed on the specific sorbent at a constant temperature. So, the study of adsorption isotherms is of importance in the design of adsorption systems to describe the adsorption mechanism. The most widely used models are the Langmuir and Freundlich adsorption isotherm models. The equations are given below:

Langmuir equation [35]:

$$\frac{C_e}{q_e}=\frac{1}{X_m K_L}+\frac{1}{X_m}C_e \tag{5}$$

where q_e is the amount of metal per unit of KMTO at equilibrium (mg/g); K_L is the constant related to the affinity of the binding sites (L/mg); X_m is the maximum amount of metal ion absorbed by per unit of KMTO (mg/g); C_e is the equilibrium concentration (mg/L).

Freundlich equation [35]:

$$\lg q_e=\lg K_F+\frac{1}{n}\lg C_e \tag{6}$$

where K_F is the Freundlich constant related to adsorption capacity; n is the Freundlich constant related to adsorption intensity.

The linear fits of these two isotherm models and the values of the isotherm constants are shown in Fig. 6. The Langmuir isotherm assumes that the monolayer adsorption occurs on specific homogeneous sites and each site can hold only one adsorbate molecule/ion (the adsorbed layer is one molecule in thickness). Besides, all sites are equivalent and there is no interaction between adsorbed molecules/ions. The Freundlich equation is an empirical equation used to describe the heterogeneous systems. The adsorption energy of a metal ion binding to a site depends on whether the adjacent sites are occupied [4,6,8,36]. For KMTO, its lepidocrocite structure is assumed to be high degree of ion exchange and the adsorption environment in KMTO may be viewed as a homogeneous system. However, the adsorption caused a disorder in the pore structure of the surfaces, resulting in an environmental change into a heterogeneous system. Accordingly, the equilibrium adsorption data are fitted into both the models of Langmuir and Freundlich because of both fitting curves are similar regarding to R^2. However, Freundlich model yields a slightly better fit (R^2=0.9918) than Langmuir model (R^2=0.9828). Therefore, the Cu(II) adsorption by KMTO can be mainly viewed as a multilayer adsorption and the majority of active sites on KMTO can be considered to be heterogeneously distributed. Moreover, the value of $1/n$ is less than 1, indicating a high adsorption intensity [37]. From q_m, the maximum adsorption capacity for Cu(II) is calculated as 290.697 mg/g. Compared with several other adsorbents in the literature presented in Table 1 [6,38−45], it is apparent that KMTO has much higher adsorption capacities for Cu(II) ions than other materials. So, KMTO is a promising adsorption material for the effective removal of copper ions from polluted water.

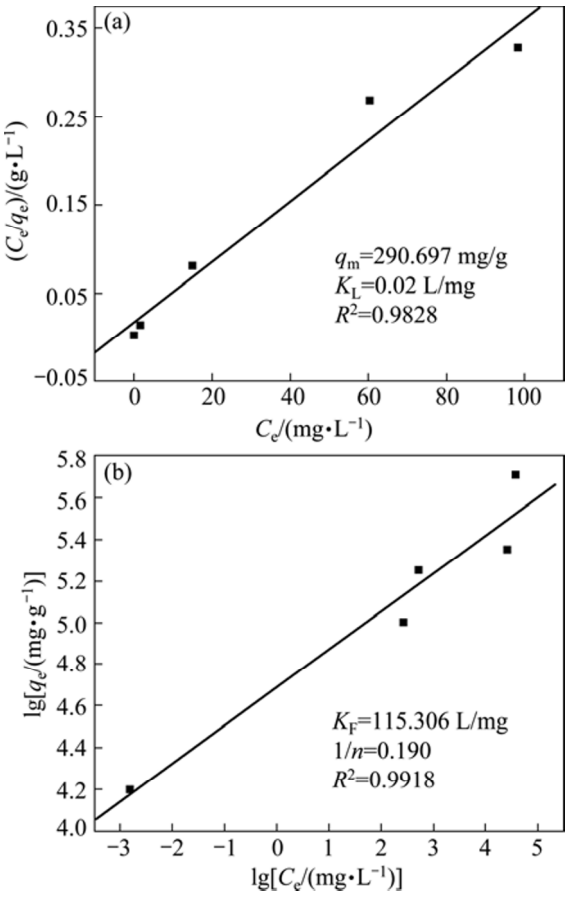

Fig. 6 Langmuir isotherm (a) and Freundlich isotherm (b) fitting curves for adsorption of Cu(II) ions with different initial concentrations at pH=3.0 and adsorption time of 6 h

3.3.5 Characterization of KMTO after adsorption

Figure 7 shows the TEM image of KMTO after adsorption at pH=3.0. It can be found that the edge and the surface of KMTO are rough, and some cracks are also found in the plates. According to previous work [19,46], the $K_{0.8}Mg_{0.4}Ti_{1.6}O_4$ plates would partially

Table 1 Comparison of maximum capacities of some adsorbents for Cu(II) ions from aqueous solution

Sorbent	Particle size/μm	Surface area/($m^2\cdot g^{-1}$)	pH	Adsorption time/h	Maximum adsorption capacity/($mg\cdot g^{-1}$)	Ref.
Grafted silica	61−190		5.5−6	6	0.1817	6
Sawdust	250−290		7	6	1.79	38
Olive stone waste	750−1500		5.5−6	1	2.03	39
Calcined phosphate (CP)	12−63	1−2	5	2	29.8	40
Manganese coated activated carbon		12.66	4	24	39.48	41
Chitosan	<250		6	1	80.71	42
Titanate nanotubes (TNT)		221.8	5	1	120	43
Kaolinite-supported zero-valent iron		9.6		24	140	44
Titanate nanofibers $Na_xH_{2-x}Ti_3O_7$		203.83		6	167.224	45
KMTO	0.3−5		3	6	290.697	This work

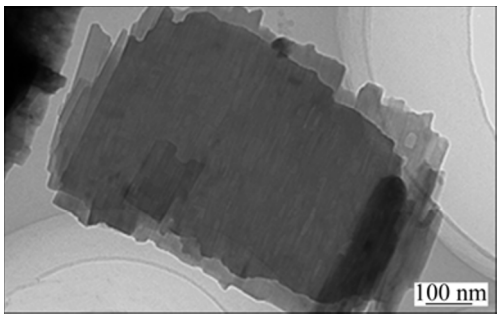

Fig. 7 TEM image of sample after treating in 100 mg/L $Cu(OH)_2$ solution at 30 °C and pH=3.0

delaminate to form cracks under acid treatment, which may expectedly provide abundant active sites and thereby make it possible to absorb more target heavy ions onto the surfaces [18, 46]. But it is also possible that the flexible sheets have creased to some extent on the surface. As a result, $Cu(OH)_2$ solution would be easily absorbed into the slits of titanate plates due to the capillary force, which enables the adsorption for Cu(II) ions [19]. Hence, it is speculated that the removal of Cu(II) ions with KMTO is a combination mechanism of cation exchange and physical adsorption.

Table 2 shows the lattice constants of the two phases before and after adsorption which are obtained from the database of the PDF standard cards. The finial ion-exchange product phase is indexed to be $H_2Ti_2O_5(H_2O)$ with similar lepidocrocite-type. Theoretically, there is an interspacing expansion from 0.782 to 0.904 nm and volume expansion from 178.17 to 204.54 Å^3, which are ascribed to "osmotic swelling" induced by the insert of structural water and H_3O^- [16]. The change of the lattice parameters can be interpreted in terms of random gliding of the host layers along *a* axis, which may be caused by the substitution of Mg^{2+} for H^+. As the ionic radius of Cu(II) ions is larger than that of Mg^{2+} ions, H^+ ions are preferentially substituted by Mg site of the hosts. During the ion exchange process in layers, protons compete with Cu(II) ions to occupy the adsorption sites of KMTO, especially in solution with low pH. However, even though H^+ ions preferentially gain access to active sites, the resulting expansion of interlayer space also provides better accessibility for Cu^{2+} to enter into layers. It can be observed that both phases are orthorhombic, the space along *c* axis does not change but that of *a* axis is different, indicating the disorder of the structure.

Table 2 Lattice constants of final phases after adsorption of Cu(II) ions

Phase	*a*/ Å	*b*/ Å	*c*/ Å	*d*/ nm	(*hkl*)	Volume/ Å^3
$K_{0.8}Mg_{0.4}Ti_{1.6}O_4$	3.821	15.641	2.981	0.782	(020)	178.17
$H_2Ti_2O_5$ (H_2O)	18.03	3.784	2.988	0.904	(200)	204.54

KMTO is an effective and environmental adsorption material for the removal of copper ions from wastewater. The effectiveness of removal of other heavy metal ions by using platy KMTO needs to be investigated further.

4 Conclusions

Platy $K_{0.8}Mg_{0.4}Ti_{1.6}O_4$ crystals were successfully prepared by flux method. The KMTO powders exhibit very high reaction efficiency in the removal of copper ions from polluted water. The combination of the excellent ion-change properties and the rough surface morphology are the main reasons for the high reaction capability in removal of heavy metals. About 99.9% of Cu(II) ions can be removed after 350 min. The maximum Cu(II) ions uptake calculated is 290.697 mg/g, which is much higher than that of many other low-cost and commercially available adsorbents. The kinetics of adsorption for different Cu(II) initial concentrations can be described by pseudo-second-order kinetic model. And the adsorption isothermal data can be well interpreted by the Freundlich equation. As a consequence, this work has provided a new candidate adsorbent for the removal of Cu(II) ions from wastewater.

References

[1] EREN E. Removal of copper ions by modified Unye clay, Turkey [J]. Journal of Hazardous Materials, 2008, 159: 235−244.

[2] SAĞ Y, AKTAY Y. Kinetic studies on sorption of Cr(VI) and Cu(II) ions by chitin, chitosan and Rhizopus arrhizus [J]. Biochemical Engineering Journal, 2002, 12: 143−153.

[3] JUSTI K C, FVERE V T, LARANJEIRA M, NEVES A, PERALTA R A. Kinetics and equilibrium adsorption of Cu(II), Cd(II), and Ni(II) ions by chitosan functionalized with 2 [-bis-(pyridylmethyl) aminomethyl]-4-methyl-6-formylphenol [J]. Journal of Colloid and Interface Science, 2005, 291: 369−374.

[4] RAHMAN M S, ISLAM M R. Effects of pH on isotherms modeling for Cu(II) ions adsorption using maple wood sawdust [J]. Chemical Engineering Journal, 2009, 149: 273−280.

[5] ÖZER G, ÖZCAN A, ERDEM B, ÖZCAN A S. Prediction of the kinetics, equilibrium and thermodynamic parameters of adsorption of copper (II) ions onto 8-hydroxy quinoline immobilized bentonite [J]. Colloids and Surfaces A: Physicochemical and Engineering Aspects, 2008, 317: 174−185.

[6] CHIRON N, GUILET R, DEYDIER E. Adsorption of Cu(II) and Pb(II) onto a grafted silica: Isotherms and kinetic models [J]. Water Research, 2003, 37: 3079−3086.

[7] LIANG Sha, GUO Xue-yi, FENG Ning-chuan, TIAN Qing-hua. Application of orange peel xanthate for the adsorption of Pb^{2+} from aqueous solutions [J]. Journal of Hazardous Material, 2009, 170: 425−429.

[8] ZHOU Y T, BRANFORD W C, NIE H L, ZHU L M. Adsorption mechanism of Cu^{2+} from aqueous solution by chitosan-coated magnetic nanoparticles modified with alpha-ketoglutaric acid [J]. Colloids Surface B: Biointerfaces, 2009, 74: 244−252.

[9] RENGARAJ S, JOO C K, KIM Y, YI J. Kinetics of removal of

chromium from water and electronic process wastewater by ion exchange resins: 1200H, 1500H and IRN97H [J]. Journal of Hazardous Material, 2003, 102: 257−275.

[10] BHATTACHARYYA K G, GUPTA S S. Adsorption of a few heavy metals on natural and modified kaolinite and montmorillonite: A review [J]. Advances in Colloid and Interface Science, 2008, 140: 114−131.

[11] SMIČIKLAS I, DIMOVIĆ S, PLEĆAŠ I, MITRIĆ M. Removal of Co^{2+} from aqueous solutions by hydroxyapatite [J]. Water Research, 2006, 40: 2267−2274.

[12] YANTASEE W, RUTLEDGE R D, CHOUYYOK W, SUKWAROTWAT V, ORR G, WARNER C L, WARNER M G, FRYXELL G E, WIACEK R J, TIMCHALK C, ADDLEMAN R S. Functionalized nanoporous silica for the removal of heavy metals from biological systems: Adsorption and application [J]. ACS Applied Materials & Interfaces, 2010, 2: 2749−2758.

[13] PAN Bing-jun, QIU Hui, PAN Bing-cai, NIE Guang-ze, XIAO Li-li, LÜ Lu, ZHANG Wei-ming, ZHANG Quan-xing, ZHENG Shou-rong. Highly efficient removal of heavy metals by polymer-supported nanosized hydrated Fe(III) oxides: Behavior and XPS study [J]. Water Research, 2010, 44: 815−824.

[14] WANG S B, ARIYANTO E. Competitive adsorption of malachite green and Pb ions on natural zeolite [J]. Journal of Colloid and Interface Science, 2007, 314: 25−31.

[15] REID A D, MUMME W G, WADSLEY A D. A new class of compound $M_x^+A_x^{3+}Ti_{2-x}O_4$ ($0.60<x<0.80$) typified by $Rb_xMn_xTi_{2-x}O_4$ [J]. Acta Crystallographica, 1968, 24: 1228−1233.

[16] ELTONI A M, YIN S, SATO T. UV shielding performance enhancement of CaO doped ceria by coupling with plate-like $K_{0.8}Li_{0.27}Ti_{1.73}O_4$ [J]. Journal of Materials Science, 2008, 43: 2411−2417.

[17] ZHANG P L, LIU X W, YIN S, SATO T. Enhanced visible-light photocatalytic activity in $K_{0.81}Ti_{1.73}Li_{0.27}O_4/TiO_{2-x}N_y$ sandwich-like composite [J]. Applied Catalysis B: Environmental, 2010, 93: 299−303.

[18] LAGALY G, BENEKE K. Intercalation and exchange reactions of clay minerals and non-clay layer compounds [J]. Colloid and Polymer Science, 1991, 269: 1198−1211.

[19] KIM Y I, SALIM S, HUQ M J, MALLOUK T E. Visible-light photolysis of hydrogen iodide using sensitized layered semiconductor particles [J]. Journal of the American Chemical Society, 1991, 113: 9561−9563.

[20] REPO E, M KINEN M, RENGARAJ S, NATARAJAN G, BHATNAGAR A, SILLANP M. Lepidocrocite and its heat-treated forms as effective arsenic adsorbents in aqueous medium [J]. Chemical Engineering Journal, 2012, 180: 159−169.

[21] SASAKI T, KOOLI F, IIDA M, MICHIUE Y, TAKENOUCHI S, YAJIMA Y, IZUMI F, CHAKOUMAKOS B C, WATANABE M. A mixed alkali metal titanate with the lepidocrocite-like layered structure: Preparation, crystal structure, protonic form, and acid-base intercalation properties [J]. Chemistry of Materials, 1998, 10: 4123−4128.

[22] OGAWA H, INADA K, ITOI N, TAKAHASHI S. Lepidocrosite type potassium magnesium titanate and method for production thereof, and friction material: US20030147804 [P]. 2003−08−07.

[23] BONDIOLI F, CORRADI A B, LEONELLI C, MANFREDINI T. Nanosized CeO_2 powders obtained by flux method [J]. Materials Research Bulletin, 1999, 34: 2159−2166.

[24] SONG Ni, LIU Yong, LIU Bo-wei, LIU Yan-bin, TAN Yan-ni, WEI Wei-feng, LUO Tao. Controlled synthesis of platy potassium titanates from potassium magnesium titanate [J]. RSC Advances, 2013, 3: 8326−8330.

[25] BAO Ning-zhong, FENG Xin, LU Xiao-hua, YANG Zhu-hong. Study on the formation and growth of potassium titanate whiskers [J]. Journal of Materials Science, 2002, 37: 3035−3043.

[26] BANFIELD J F, WELCH S A, ZHANG H, EBERT T T, PENN R L. Aggregation-based crystal growth and microstructure development in natural iron oxyhydroxide biomineralization products [J]. Science, 2000, 289: 751−754.

[27] PENN R L, BANFIELD J F. Imperfect oriented attachment: Dislocation generation in defect-free nanocrystals [J]. Science, 1998, 281: 969−971.

[28] DEMIRBAŞ Ö, KARADAĞ A, ALKAN M, DOĞAN M. Removal of copper ions from aqueous solutions by hazelnut shell [J]. Journal of Hazardous Materials, 2008, 153: 677−684.

[29] HO Y S, MCKAY G. Pseudo-second order model for sorption processes [J]. Process Biochemistry, 1999, 34: 451−465.

[30] DOĞAN M, ÖZDEMIR Y, ALKAN M. Adsorption kinetics and mechanism of cationic methyl violet and methylene blue dyes onto sepiolite [J]. Dyes and Pigments, 2007, 75: 701−713.

[31] CHIOU M, LI H. Adsorption behavior of reactive dye in aqueous solution on chemical cross-linked chitosan beads [J]. Chemosphere, 2003, 50: 1095−1105.

[32] BABEL S, KURNIAWAN T A. Cr(VI) removal from synthetic wastewater using coconut shell charcoal and commercial activated carbon modified with oxidizing agents and/or chitosan [J]. Chemosphere, 2004, 54: 951−967.

[33] LI Jia-xing, HU Jun, SHENG Guo-dong, ZHAO Gui-xia, HUANG Qing. Effect of pH, ionic strength, foreign ions and temperature on the adsorption of Cu(II) from aqueous solution to GMZ bentonite [J]. Colloids and Surfaces A: Physicochemical and Engineering Aspects, 2009, 349: 195−201.

[34] PETROV S A, GRIGOR'EVA L, SINEL'SHCHIKOVA O Y, SINEL'SHCHIKOVA T Y, GUSAROV V. Synthesis and study of isomorphous miscibility limits of crystalline phases with a hollandite-type tunnel structure in the Cs_2O (MeO)–Al_2O_3–TiO_2 (Me=Ba, Sr) systems [J]. Glass Physics and Chemistry, 2003, 29: 316−321.

[35] YAN Han, YANG Ling-yun, YANG Zhen, YANG Hu, LI Ai-min, CHENG Rong-shi. Preparation of chitosan/poly (acrylic acid) magnetic composite microspheres and applications in the removal of copper (II) ions from aqueous solutions [J]. Journal of Hazardous Materials, 2012, 229−230: 371−380.

[36] SASAKI T, WATANABE M. Osmotic swelling to exfoliation: Exceptionally high degrees of hydration of a layered titanate [J]. Journal of the American Chemical Society, 1998, 120: 4682−4689.

[37] HUANG Ji-quan, CAO Yong-ge, LIU Zhu-guang, DENG Zhong-hua, TANG Fei, WANG Wen-chao. Efficient removal of heavy metal ions from water system by titanate nanoflowers [J]. Chemical Engineering Journal, 2012, 180: 75−80.

[38] YU B, ZHANG Y, SHUKLA A, SHUKLA S S, DORRIS K L. The removal of heavy metal from aqueous solutions by sawdust adsorption: Removal of copper [J]. Journal of Hazardous Material, 2000, 80: 33−42.

[39] FIOL N, VILLAESCUSA I, MART NEZ M, MIRALLES N, POCH J, SERAROLS J. Sorption of Pb(II), Ni(II), Cu(II) and Cd(II) from aqueous solution by olive stone waste [J]. Separation and Purification Technology, 2006, 50: 132−140.

[40] AKLIL A, MOUFLIH M, SEBTI S. Removal of heavy metal ions from water by using calcined phosphate as a new adsorbent [J]. Journal of Hazardous Material, 2004, 112: 183−190.

[41] TIWARI D, LEE S M. Biomass-derived materials in the remediation of heavy-metal contaminated water: Removal of cadmium (II) and copper (II) from aqueous solutions [J]. Water Environment Research, 2011, 83: 874−881.

[42] WAN N W, ENDUD C, MAYANAR R. Removal of copper (II) ions from aqueous solution onto chitosan and cross-linked chitosan beads [J]. Reactive and Functional Polymers, 2002, 50: 181−190.

[43] LIU S S, LEE C K, CHEN H C, WANG C C, JUANG L C. Application of titanate nanotubes for Cu(II) ions adsorptive removal from aqueous solution [J]. Chemical Engineering Journal, 2009, 147: 188−193.

[44] UZUM C, SHAHWAN T, EROGLU A, HALLAM K, SCOTT T, LIEBERWIRTH I. Synthesis and characterization of kaolinite-supported zero-valent iron nanoparticles and their application for the removal of aqueous Cu^{2+} and Co^{2+} ions [J]. Applied Clay Science, 2009, 43: 172−181.

[45] LI Nian, ZHANG Li-de, CHEN Yong-zhou, TIAN Yue, WANG Hui-min. Adsorption behavior of Cu(II) onto titanate nanofibers prepared by alkali treatment [J]. Journal of Hazardous Material, 2011, 189: 265−272.

[46] BESSELINK R, STAWSKI T M, CASTRICUM H L, BLANK D H, TEN ELSHOF J E. Exfoliation and restacking of lepidocrocite-type layered titanates studied by small-angle X-ray scattering [J]. The Journal of Physical Chemistry C, 2010, 114: 21281−21286.

片状钛酸镁钾的制备及其去除污水中铜离子的应用

谭彦妮，宋 旎，刘 咏，罗 涛，窦玉海，张 青，刘倩楠，罗兰兰

中南大学 粉末冶金国家重点实验室，长沙 410083

摘 要：采用熔盐法制备片状钛酸镁钾($K_{0.8}Mg_{0.4}Ti_{1.6}O_4$, KMTO)，并将其应用于去除污水中的 Cu(II)离子。分别采用 XRD、SEM 和 TEM 等技术对样品的晶相组成、形貌和结构进行表征。研究不同 pH 值和初始铜离子浓度对铜离子吸附行为的影响。结果显示，铜离子的最大饱和吸附量可达到 290.67 mg/g，采用 KMTO 可以去除溶液中几乎 99.9% 的铜离子。该结果优于其他文献报道的离子去除剂的结果。KMTO 对铜离子的吸附动力学研究结果显示，钛酸镁钾对铜离子的吸附符合拟二级反应动力学方程，而其吸附等温数据可以用 Freundlich 方程很好地进行拟合(R^2=0.991)。研究结果表明，片状钛酸镁钾在处理污水中的重金属离子方面具有很好的应用前景，为片状钛酸镁钾开辟了新的应用领域。

关键词：钛酸镁钾；废水；铜离子；去除；吸附动力学；熔盐法

(Edited by Wei-ping CHEN)